HF coherent scatter radar observations of ionospheric convection during magnetospheric substorms

Mark Lester

*Department of Physics and Astronomy, University of Leicester, Leicester,
LE1 7RH, U.K.*

Abstract: Observations of ionospheric convection have proven to be extremely valuable in understanding the interaction between the solar wind and the magnetosphere, particularly through the process of magnetic reconnection. In addition, the response of ionospheric convection to substorm activity can provide insight into the mechanisms associated with magnetospheric substorms. In this paper we review observations of ionospheric convection during all phases of the substorm made by HF coherent scatter radars such as those that form the Super Dual Auroral Radar Network (SuperDARN). By concentrating on HF coherent scatter radar observations we stress the importance of ion velocity measurements rather than the conductance controlled ionospheric electrojets. The observations reviewed in this paper demonstrate a number of key results. Following long periods of quiet magnetic activity usually associated with intervals of northward interplanetary magnetic field (IMF), the region of radar backscatter in the dusk local time sector moves equatorward. Based upon this motion of the radar backscatter and a model for the reconnection rate at the dayside magnetopause, it is possible to estimate the length of the reconnection line at the magnetopause, which is found to vary between 12 and 27 R_E. At expansion phase onset, the scatter can often be lost for short periods of time due to absorption of the HF radio wave. There is also evidence that convection vortices in the post noon local time sector relax at the time of expansion phase onset, which hints at a global response to the expansion phase onset. During the latter part of the expansion phase bursts of flow are seen to occur which have repetition rates similar to flux transfer events (FTEs) and current vortices similar to the ionospheric signatures of FTEs. HF coherent scatter radars also play a key role in multi-instrument studies of magnetospheric substorms, for example providing near continuous observations of the convection reversal boundary as a proxy for the polar cap boundary. The recovery phase is the least studied of the various phases but there are key observations of omega bands in the post midnight local time sector, which also hint at the expansion phase being a global phenomenon. The paper concludes with some suggestions of how HF coherent scatter radars will be used in future studies of convection during substorms.

1. Introduction

Coupling between the interplanetary medium (solar wind) and the Earth's magnetosphere is mainly controlled by reconnection of the interplanetary magnetic field (IMF) with the geomagnetic field (Dungey, 1961; Cowley, 1984). This process drives convection within the magnetosphere, such that newly opened magnetic flux is moved into the region of open flux, often referred to as the polar cap, and subsequently added to

the lobes of the magnetic tail of the magnetosphere. At some time later in the cycle reconnection of open field lines embedded within the northern and southern tail lobes results in closed flux being transported sunwards from the tail. Although the process of reconnection at the dayside magnetopause which results in open flux is well understood (*e.g.* Cowley, 1998), the same cannot be said for reconnection in the tail. It is believed that reconnection does take place in an explosive fashion at some time during the substorm process. Observations of fast, tailward ion flows with southward magnetic fields by the Geotail satellite suggest that reconnection occurs between 20 and 30 R_{E} downtail in the pre-midnight sector (Nagai *et al.*, 1998). These fast tailward flows appear to occur a few minutes prior to Pi2 pulsation onset on the ground, a normal indicator for substorm expansion phase onset. These observations notwithstanding, when reconnection occurs at this location in the tail during the substorm is still a controversial subject. The proponents of the Near Earth Neutral Line model (NENL) suggest that reconnection of open magnetic flux in the tail is responsible for the substorm expansion phase onset (see Baker *et al.*, 1996 for a recent review). Others (*e.g.* Lui, 1996) suggest that reconnection of open flux is a response to an earlier mechanism responsible for substorm expansion phase onset and, therefore, can take place up to several tens of minutes after expansion phase onset.

Measurements of ionospheric convection, in conjunction with optical data, have proven very successful in understanding and diagnosing the reconnection process at the dayside magnetopause (*e.g.* Lockwood *et al.*, 1993; Cowley, 1998). Indeed it is far easier to observe the consequences of magnetic reconnection at the dayside magnetopause in the ionosphere than in the magnetosphere. The large volume of the magnetosphere does not allow the 'global' coverage of convection which can be achieved by ground based systems, such as coherent and incoherent scatter radars and magnetometers, in measuring convection in the ionosphere.

Our current understanding of how ionospheric convection is generated as a result of reconnection at the dayside magnetopause and in the tail is presented in Fig. 1, taken from Lockwood *et al.* (1990a). In panel a of this figure convection is generated by reconnection at the dayside magnetopause alone. The reconnection site at the magnetopause, which maps into the ionosphere is represented by the dashed part of the circle. The full part of the circle represents the boundary between open and closed magnetic flux mapped into the ionosphere. This boundary is often termed the polar cap boundary (PCB). We note that the PCB for these sketches is co-located with the convection reversal boundary (CRB), which can be used as a proxy for the PCB. Since in panel a of Fig. 1 reconnection is limited to occurring at the dayside magnetopause only, open flux is transferred into the polar cap, which then expands in size, indicated by the solid arrows in the figure. The ionospheric convection associated with the addition of this magnetic flux is the standard twin cell pattern with antisunward flow across the separatrix and sunward flow on closed field lines. It should be borne in mind that in this model the PCB is adiaroic (Siscoe and Huang, 1985), *i.e.* there is no flow across the boundary and the motion of the boundary alone is responsible for the flow in this region.

If there is reconnection only in the tail and not at the dayside magnetopause then the situation is described by Fig. 1b. Here the flow across the ionospheric footprint of the reconnection site, which is now on the nightside, is still antisunward but is out of the
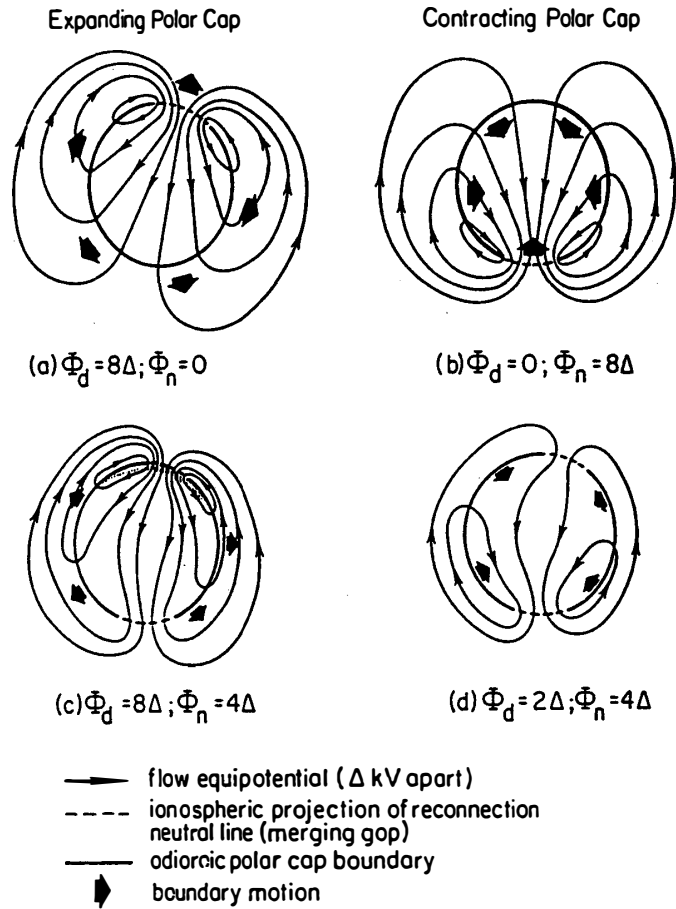
Expanding Polar Cap   Contracting Polar Cap

(a) $\Phi_d = 8\Delta; \Phi_n = 0$ (b) $\Phi_d = 0; \Phi_n = 8\Delta$

(c) $\Phi_d = 8\Delta; \Phi_n = 4\Delta$ (d) $\Phi_d = 2\Delta; \Phi_n = 4\Delta$

— flow equipotential (Δ kV apart)
---- ionospheric projection of reconnection
     neutral line (merging gap)
—— adiorcic polar cap boundary
▶ boundary motion

Fig. 1. *Sketches of ionospheric convection as a result of magnetic reconnection at the dayside magnetopause and in the tail. The circular solid line represents the polar cap boundary (PCB), while the dashed lines are the ionospheric footprints of the reconnection neutral lines, often referred to as merging gaps. The solid arrows represent the motion of the PCB (after Lockwood et al., 1990a).*

polar cap since open magnetic flux is now being closed in the tail. The twin cell convection pattern is still set up, however. The motion of the PCB is different and is seen to contract. The lower two panels of Fig. 1 give examples where the dayside reconnection rate exceeds the nightside reconnection rate (Fig. 1c) and vice versa (Fig. 1d). In the former case the PCB is expanding on average while in the latter it is contracting. This model is often described as the expanding contracting polar cap (ECPC) model.

Since the response to reconnection at the dayside has been successfully diagnosed within the constraints of this model, it is expected to act as a good framework for nightside reconnection. Thus, this paper reviews observations of ionospheric convection during substorms in order to investigate whether we can understand reconnection processes in the tail. Ionospheric convection has been measured directly by a number of techniques, *e.g.* low altitude spacecraft electric field and ion velocity instruments, incoherent scatter radars and VHF and HF coherent scatter radars, and indirectly by estimating the current distribution from magnetometer data. Here we concentrate on observations made with HF coherent scatter radars, such as those that form the Super

Dual Auroral Radar Network (SuperDARN) (Greenwald *et al.*, 1995). It is pertinent at this time to review the current status of our observations with HF coherent scatter radars as the SuperDARN array is now well placed to make almost global observations of ionospheric convection and substorms are a global phenomenon. Furthermore, the HF coherent scatter radars provide an opportunity to measure the ionospheric velocities directly, which other global networks of instruments, such as magnetometers are unable to do.

Many observations have been made during substorms with magnetometers and it is worthwhile at this juncture considering the observations of the current systems that flow during substorms. It is well known that the ionospheric current systems at high latitudes can be divided into two basic forms, the so-called DP1 and DP2 current systems (*e.g.* Kamide and Baumjohann, 1993). The latter current system is also referred to as the convection electrojets, consisting of an eastward electrojet on the dusk flank of the ionosphere and a westward eletrojet on the dawn flank. These currents are partially fed by a series of downward field aligned currents on the dayside and upward field aligned currents on the nightside, although some of the current closes entirely within the ionosphere. These electrojets can be considered to be the counterpart of the return flow associated with the reconnection driven flows in Fig. 1, although it is generally accepted that they are mainly driven by dayside reconnection. Following substorm expansion phase onset an enhanced westward electrojet in the midnight sector occurs as part of the substorm current wedge (McPherron *et al.*, 1973) or the DP1 current.

The synthesis of these current systems has primarily been made from analysis of ground based magnetometer records (*e.g.* Kamide and Kokubun, 1996). The currents flowing in the E region of the ionosphere, however, will have contributions from two parameters, conductivity and electric fields, and the relative strength of these two parameters in local time and during substorms is very complex. This is demonstrated by the observations presented in Fig. 2 (based upon data discussed by Lester *et al.*, 1996) where simultaneous measurements by EISCAT of the height integrated Hall and Pedersen conductivity (Fig. 2a), the north-south and east-west electric field (Fig. 2b) and the east-west current (Fig. 2c) are presented. The interval shown in Fig. 2 consists of at least 7 Pi2 pulsations with the first at 1936 UT probably related to a pseudo break-up and the main expansion phase onset at 2018 UT. The east-west current (Fig. 2c) is highly variable, particularly after the expansion phase onset, and the variability is in general mainly due to the height integrated Hall conductivity rather than the electric field. The currents, therefore, respond primarily to the conductivity changes rather than electric fields, which would result in convection flows as well as currents. Thus, HF coherent scatter radars, which make direct measurements of ionospheric convection, play an important role in diagnosing the ionospheric electric fields during all phases of the substorm.

The remainder of this paper reviews current work with HF coherent scatter radars on substorm associated ionospheric convection. Initially, however, an overview of the present HF coherent scatter radars available is provided. The review of observations is divided into 4 sections, those made during the growth phase, at expansion phase onset, later in the expansion phase and finally the recovery phase observations. The paper is concluded with some discussion of outstanding problems which it is believed
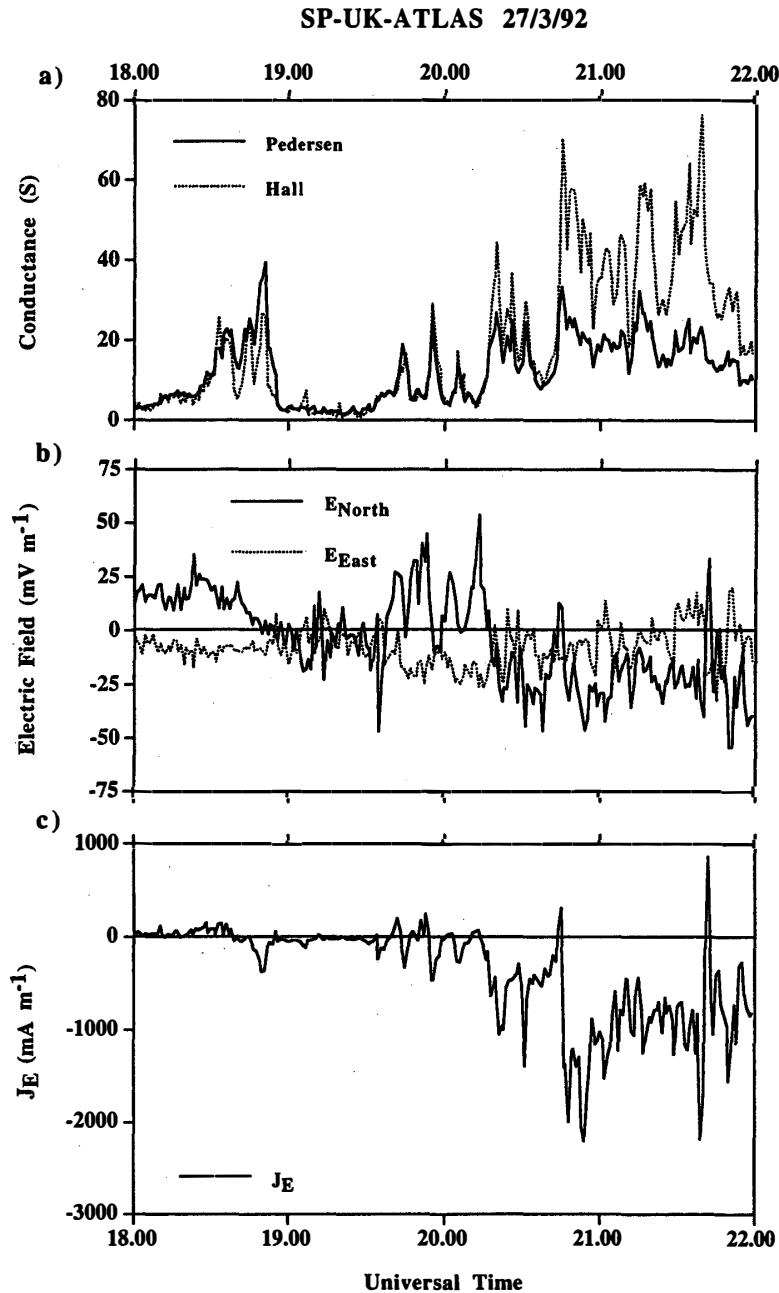
SP-UK-ATLAS 27/3/92

Fig. 2. Time series of the height integrated Hall and Pedersen conductivity (panel a), the north-south and east west electric field (panel b) and the east-west current (panel c) for the interval 18–22 UT measured by EISCAT on 27 March 1992.

SuperDARN will help to resolve.

2. HF coherent scatter radars

Coherent scatter radars rely on the Bragg scattering of radio waves by small-scale, ionospheric, magnetic field-aligned irregularities. Conditions for irregularity generation are not always satisfied and thus a coherent scatter radar does not always observe radar

backscatter over the complete radar field of view. The generation of irregularities is a complex topic and is not discussed further here. The reader is referred to excellent reviews by Fejer and Kelly (1980) and Haldoupis (1989). Since the irregularities are field-aligned, for direct backscatter, *i.e.* co-located transmitter and receiver, there is a geometrical constraint that the radar wave vector must be orthogonal to the magnetic field. Thus, since many early high-latitude coherent scatter radars operated at VHF and UHF frequencies, these radars received backscatter from the auroral E region. Furthermore, it was impossible to satisfy exactly the orthogonality condition at ionospheric altitudes at latitudes greater than approximately 70°.

HF coherent scatter radars overcome this constraint by using the natural refraction of the ionosphere to achieve orthogonality in both the E and F regions. Furthermore, such radars utilise the "over the horizon" propagation and therefore can achieve orthogonality over a larger range of distances, thereby increasing the radar field of view. There are effects on propagation, however, which can limit the performance of these radars. At HF frequencies absorption of the radio wave is largest and, therefore, the signal can be lost if there is enhanced D and/or E region ionisation. This is discussed further in Section 4. Also, for a given frequency a minimum electron density is required for the wave to propagate, but this can be overcome by having a system capable of operating at different frequencies.

The current generation of HF coherent scatter radars, which form SuperDARN (Greenwald *et al.*, 1995), is based upon the Goose Bay radar (Greenwald *et al.*, 1985), although there have been subsequent technical developments to the basic system. There are currently 6 operating radars in the northern hemisphere and 5 in the southern hemisphere with 4 more under construction, 3 of which will be deployed in the north and 1 in the south. The fields of view of the operational radars (as at October 1999) are given in Fig. 3, demonstrating the overlapping nature of the fields of view of certain radars and the large coverage in both hemispheres. Each radar uses an electronically steered, phased array to point in 16 different directions with a typical beamwidth, which is frequency dependent, of 3–4°. The angular spacing between beam directions is 3.25° and the total angular coverage is ~52°. The main standard mode of operation is currently a 16 beam scan with 7 s integration time along each beam and the scans are synchronised to start on successive 2 min boundaries. A higher time resolution common mode operates with 3 s integration time on each beam direction and the scans are synchronised on 1 min boundaries. The radars are, however, very flexible and can, therefore, operate in many different modes, although for at least 50% of the time the radars operate in one of the common modes described above.

Since the start of August 1995 the SuperDARN radars have operated using a pulse sequence of 7 pulses which has a total length of 67.2 ms. The pulses have a basic length of 300 μs and a basic lag separation of 2400 μs. The pulses are distributed within the pulse sequence such that a total of 18 lags are calculated. The basic pulse length of 300 μs corresponds to 45 km range gates, although this can be improved to 15 km range gates if necessary by reducing the pulse length to 100 μs. From the basic pulse sequence an autocorrelation function (ACF) can be computed from which a spectrum can be calculated as well as the basic measured parameters. These are backscatter power, Doppler (line-of-sight) velocity and spectral width. Of these the most used is the
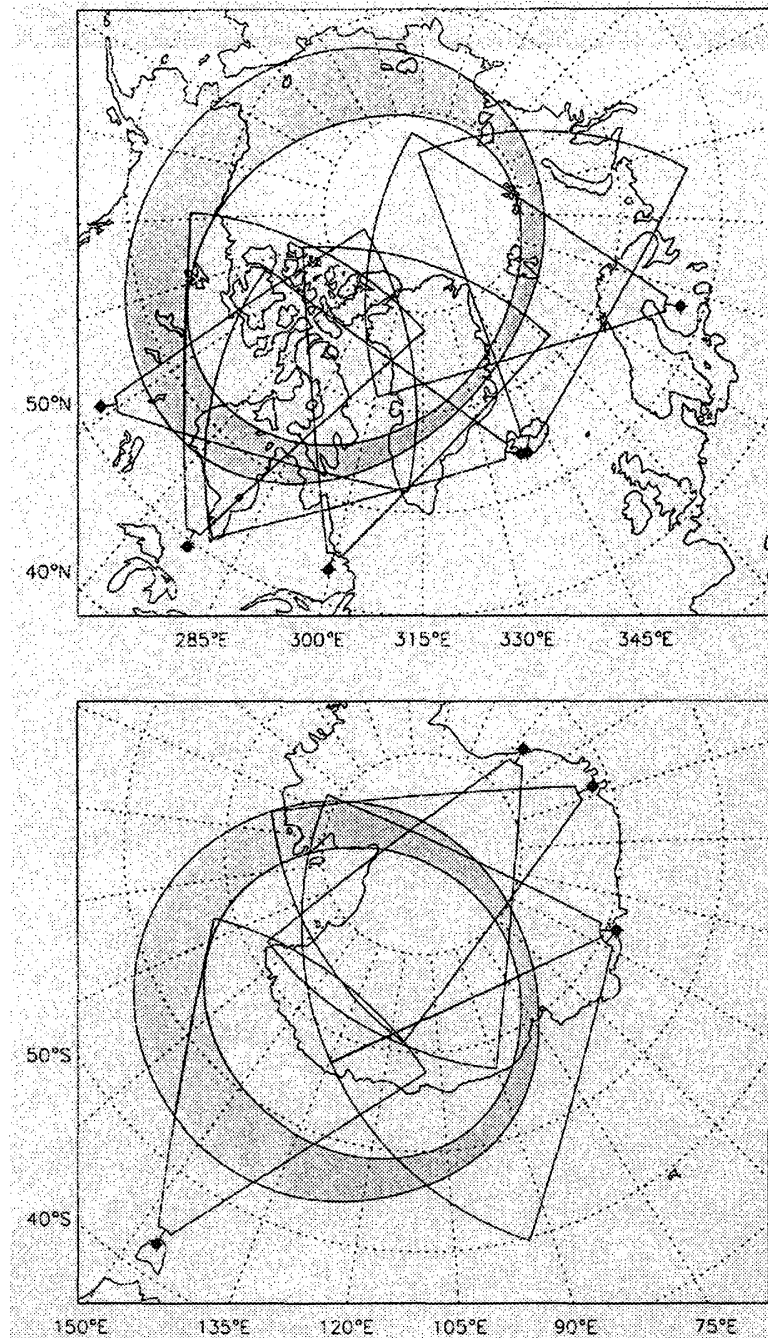
Fig. 3. The fields of view of the operational SuperDARN radars (as of October 1999). The top panel gives the northern hemisphere radars and the lower panel the southern hemisphere radars.

Doppler velocity. Since radar fields of view overlap, coincident measurements of velocity by two radars allow the 2-dimensional velocity vector perpendicular to the magnetic field to be calculated. Further, more sophisticated analysis of the velocity data is also possible such as using the map potential model of Ruohoniemi and Baker (1998).

3. Substorm growth phase

It is generally accepted that the substorm growth phase is an interval of overall magnetic flux addition to the polar cap. In terms of Fig. 1, or the ECPC model, the polar cap expands as a result of the dayside reconnection rate being higher than the nightside reconnection rate. There is evidence from global optical images that the polar cap area, *i.e.* that area devoid of optical luminosity within the poleward boundary of the auroral oval, does increase during the growth phase (*e.g.* Brittnacher *et al.*, 1999). HF coherent scatter radar observations, in particular the variation of the equatorward boundary of the radar backscatter (Lewis *et al.*, 1997, 1998a; Yeoman *et al.*, 1999), support this observation.

Figure 4 illustrates the effect with radar data from the Goose Bay and Halley radars which have approximately conjugate fields of view. The two panels of Fig. 4 are latitude-time-velocity plots for the interval 00–04 UT on 17 March 1996. Concentrating first on the Goose Bay data, the regions of scatter between 0000 and 0130 UT extended from ~70° to 77° magnetic latitude with perhaps a slight equatorward motion of less than 1° of magnetic latitude (Fig. 4a). Following 0130 UT, however, the equatorward boundary of the scatter moved rapidly equatorward to 64° magnetic latitude in the next 30 min. This rapid motion was not simply caused by the rotation of the radar field of view beneath a static auroral oval, as demonstrated by the location of the average auroral oval represented by the two thin solid lines in each panel of Fig. 4. The lower panel of Fig. 4 demonstrates a similar equatorward motion in the southern hemisphere over the same time interval, following the same behaviour between 0000 and 0130 UT. The IMF B_z component turned negative at ~0120 UT at the dayside magnetopause and remained negative until at least 0400 UT apart from a brief, <10 min, interval near 0230 UT. Ground based magnetometer data from both hemispheres indicate a pseudo break-up occurred at 0150 UT and a full substorm expansion phase onset at 0230 UT. Thus the equatorward motion of the radar backscatter occurred during the substorm growth phase.

To investigate the cause of such equatorward motion of the region of scatter Lewis *et al.* (1998a) utilised the E_j (2) parameter (Sonnerup, 1974; Hill, 1975) which provides an estimate of the reconnection rate at the dayside magnetopause. By making a number of assumptions Lewis and co-workers demonstrated that the equatorward motion of the radar backscatter was well predicted by a simple motion of the expansion of a spherical polar cap. The thicker line starting at 0130 UT in each panel of Fig. 4 is the prediction for the interval discussed here. It should be noted that the length of the magnetopause X line required to match the predictions to the observations was typically 12 R_E (Lewis *et al.*, 1998a), although for the event in Fig. 4 it was estimated to be 27 R_E. Thus these observations provide quantitative evidence in support of the ECPC model in terms of the effect on the location of the HF radar backscatter.

A common feature of the 5 events discussed by Lewis *et al.* (1998a) and the event presented in Fig. 4 (Yeoman *et al.*, 1999) is that they all followed extended intervals of northward IMF. This suggests that the magnetosphere was in a state of quiescence prior to the start of the substorm growth phase. To date, events where this has not been the case have not been reported and the question arises whether the quiescent state of the magnetosphere is a necessary condition for HF coherent scatter radars to be able to make
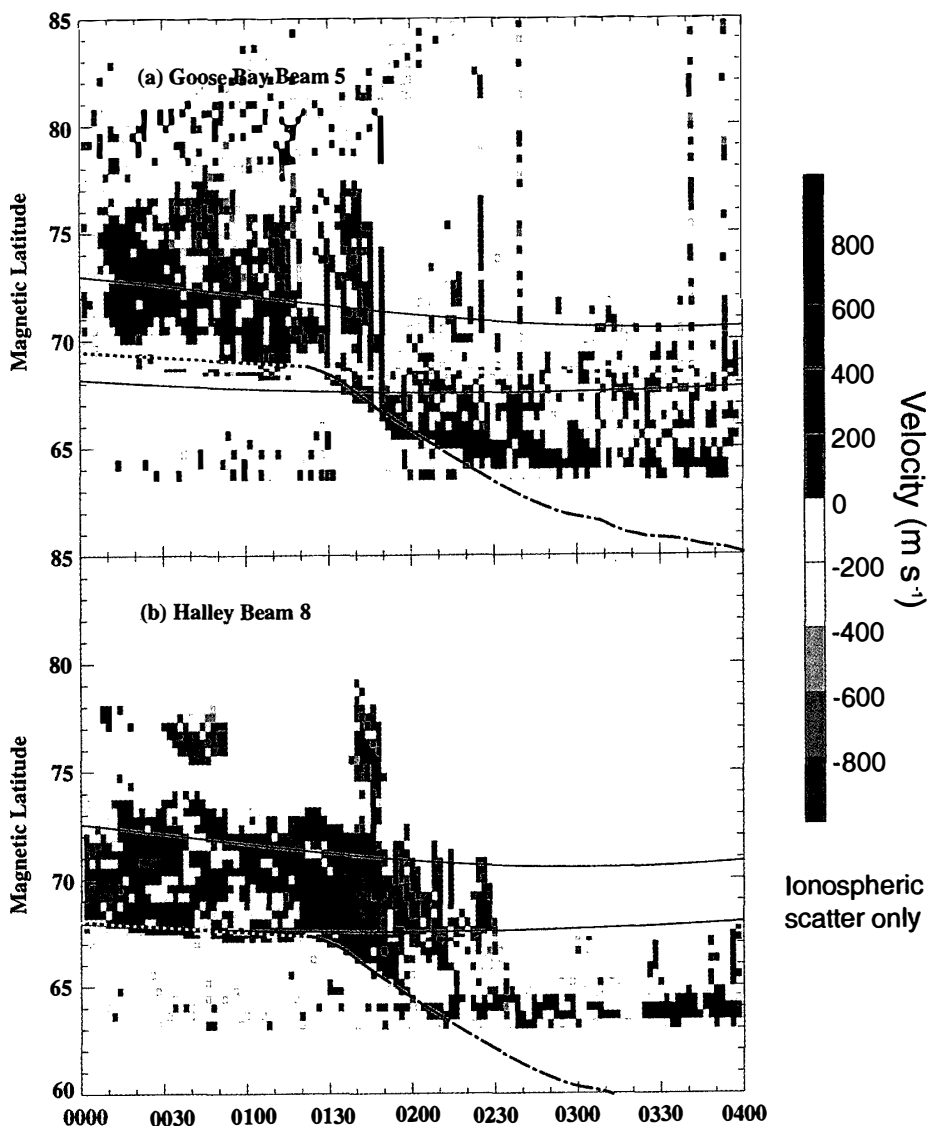
Goose Bay/Halley Velocity 17 March 1996

Fig. 4. Range Time Velocity plots from Goose Bay (top panel) and Halley (bottom panel) for the interval 00–04 UT on 17 March 1996. The thin lines represent the average auroral oval location, while the thicker dashed line represents the calculated position of the equatorward edge of the radar backscatter assuming reconnection takes place as described in the text.

these observations.

Often during the substorm growth phase one or more pseudo break-ups occur (e.g. Koskinen et al., 1993). These features have many of the characteristics of the auroral break-up at expansion phase onset without the poleward expansion of the aurora. They are typically localised in both latitudinal and local time extent. There have been a few observations by HF coherent scatter radars during pseudo break-ups (e.g. Lewis et al., 1998b; Lester et al., 1998). In the second of these two studies, Lester et al. (1998) observed a reduction in the line of sight velocity measured by the CUTLASS Finland radar close to the optical enhancement associated with two pseudo break-ups. Lewis et

al. (1998b) found increased plasma flow and current during the growth phase which was in response to what they called the DP2 electric field. They also commented that a pseudo break-up which occurred late in the growth phase was associated with a substorm current wedge electric field. The increase in plasma flow and current at that time may have been related to the superposition of these two electric fields, although the observations were not optimum for the event. These two observations appear to be discrepant and suggest that more work needs to be undertaken to understand the exact response of the convection to pseudo break-ups. One feature of the pseudo break-up which occurred in the interval presented in Fig. 4 is that it did not decrease the rate of equatorward expansion of the radar scatter. If anything, the rate may have increased following the pseudo break-up (Yeoman *et al.*, 1999).

Another feature of substorm growth phase is the appearance of convection vortices on the dayside (Greenwald *et al.*, 1996). These vortices appear to be centred near 1430–1530 MLT and 75° to 80° magnetic latitude (see Fig. 5). Here, four consecutive maps of the ionospheric convection measured by the Saskatoon-Kapuskasing and Goose Bay-Stokkseyri pairs of radars (Greenwald *et al.*, 1995) are presented. These maps cover a total time interval of just 6 min. The convection vortex centred on 15 MLT is clearly seen in the first 3 maps, but in the fourth map there is evidence that the vortex is starting to relax, which we return to in Section 4. The vortex scale size varies from a few hundred to ~1000 km and there is an associated potential drop of 5–10 kV. When observed, the vortices can remain within a radar field of view for 10–15 min while the centre of the vortex is often stationary and at most moves only a few hundred kilometres. These quasi-static features vary in intensity and are particularly intense just before expansion phase onset. Vortices in the ionospheric flow are usually considered to be directly related to field-aligned currents (*e.g.* Sofko *et al.*, 1995). Based upon typical scale sizes and flows, and assuming a value for the height integrated Pedersen conductivity, Σ_P, Greenwald *et al.* (1996) estimate the field-aligned current density associated with these quasi-static vortices can be at least 3 μA m^{-2} within a 100 km circle. This is equivalent to a total field-aligned current of ~10^5 A, which would be out of the ionosphere given the vorticity direction.

The exact magnetospheric source of these convection vortices remains unclear. Greenwald *et al.* (1996) discussed a number of potential sources such as the Kelvin-Helmholtz instability at the magnetopause, the dusk end of a split merging line, magnetospheric flux transfer events (FTEs) and direct driving by the solar wind. All of these, however, have some aspect which is not satisfactory with respect to the characteristics of the vortex. It is interesting to note that they occur preferentially in a MLT sector when there is often a region of strong auroral emission (*e.g.* Cogger *et al.*, 1977) and a statistical maximum in the energy flux of precipitating electrons at energies less than 3 keV (Evans, 1985). Furthermore, there is a minimum in the response time of the ionospheric convection to changes in the IMF at this MLT (*e.g.* Etemadi *et al.*, 1988; Khan and Cowley, 1999). With regard to substorms in general, perhaps the most intriguing aspect is the disappearance of the vortices at expansion phase onset which will be discussed further later in this paper.
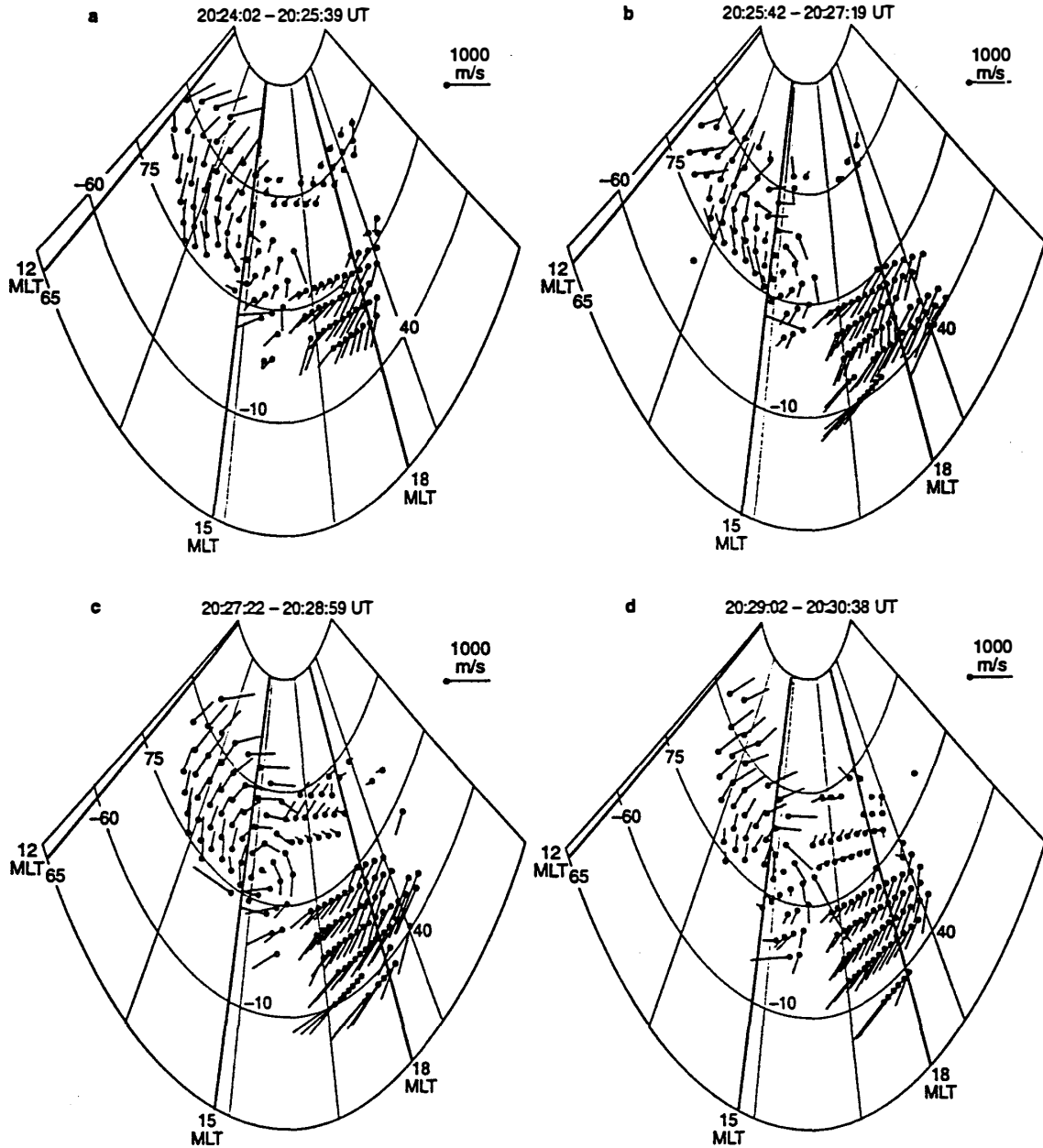
Fig. 5. Maps of the high latitude convection observed with the Saskatoon/Kapuskasing and Goose Bay/Stokkseyri pairs of radars covering the interval 2024:02 to 2030:43 UT on 19 October 1994.

4. Expansion phase onset

Expansion phase onset is characterised by rapid enhancement and large scale expansion of the nightside auroral activity which is caused by enhanced particle precipitation. Thus, the ionisation of the E-region and possibly D region, depending upon the energy of particle precipitation, increases. This increase in ionisation at these altitudes results in increased absorption of radio waves which pass through the region of ionisation due to enhanced collision frequency. Indeed, riometers which measure cosmic noise absorption (CNA), clearly observe substorm activity as an increase in absorption

(*e.g.* Ranta, 1978). This absorption can affect HF radars, as at expansion phase onset radar backscatter is often lost. This is illustrated in Fig. 4b, where after 0230 UT the time of expansion phase onset, the scatter at Halley effectively disappeared apart from some near range E-region scatter. Many other studies report such data loss following expansion phase onset (*e.g.* Lewis *et al.*, 1997, 1998a, b; Yeoman and Lühr, 1997; Lester *et al.*, 1998).

Radar backscatter is not always completely lost following expansion phase onset. In Fig. 6 line of sight velocity data from the CUTLASS Finland radar for beam 9 are presented for the interval 19–24 UT on 6 August 1995 (Yeoman and Lühr, 1997). Data from the IMAGE magnetometer stations suggest that pseudo break-ups occurred at 1952 UT and 2008 UT, while the expansion phase onset occurred at 2024 UT. There were two subsequent intensifications at 2033 UT and 2057 UT. A second substorm expansion phase onset then occurred at 2208 UT, which did not appear to be preceded by any pseudo break-up but was followed by two intensifications at 2219 UT and 2254 UT.

Just before the first expansion phase onset at 2024 UT the radar backscatter extended from 66.5° to 71.5° magnetic latitude. At expansion phase onset the scatter from the poleward most 3.5° was lost, although the equatorward boundary did move to 65° magnetic latitude. Following 2033 UT there was a gradual recovery, such that after 2045 UT the region of scatter extended from 65° to 71.5° magnetic latitude. Similarly, following the second expansion phase onset at 2208 UT scatter was lost from the poleward most 3° and the interval over which scatter was lost was ~20 min. During these two events absorption measurements by the riometer at Kilpisjarvi have provided some estimates of the region over which absorption would have affected the HF radar propagation. Detailed ray tracing of several intervals of backscatter loss at expansion
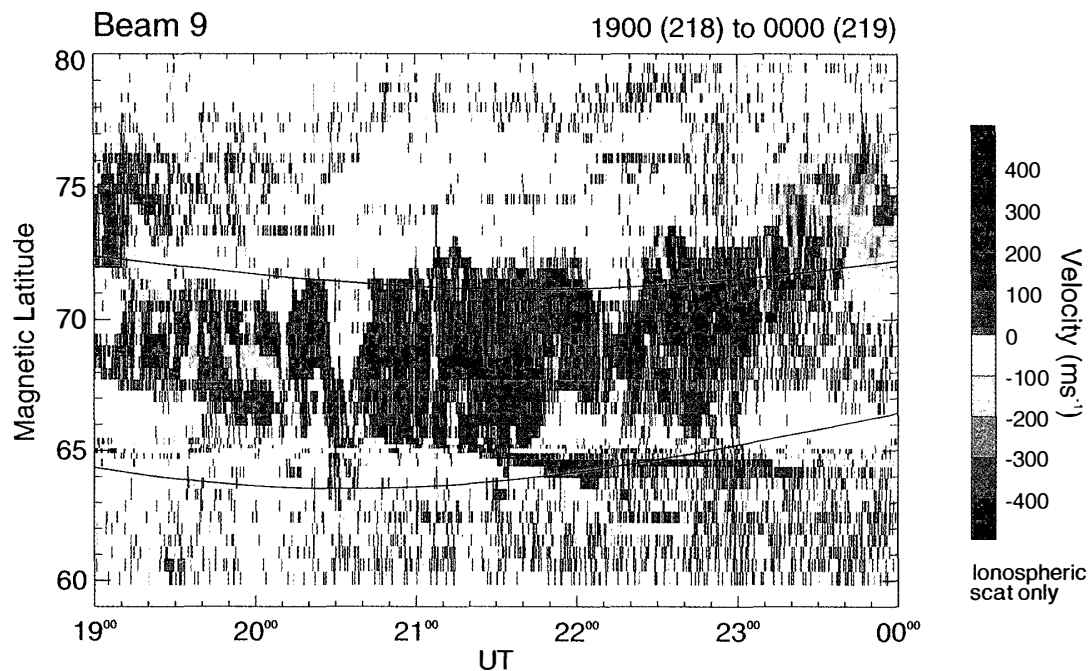

Fig. 6. Range Time Velocity plot from the Finland radar for the interval 19–24 UT on 6 August 1995. The thin lines represent the average auroral oval position.

phase onset has suggested, however, that the loss of scatter in Fig. 6 is more consistent with extra refraction of the HF radio wave. This is typically seen in other similar events as a loss of scatter with a certain range of elevation angles. For the event in Fig. 6, however, no interferometer data were available to confirm this interpretation (J. Gauld and T.K. Yeoman, private communication, 1999). Other events clearly demonstrate that the loss of scatter is due to absorption and in addition to absorption and the change in propagation conditions, small or zero electric fields will also cause scatter to be lost (*e.g.* Milan *et al.*, 1999).

Since the field of view of the HF radar is much larger than that of a riometer, then it may be possible to utilise the region over which scatter is lost to predict the location of enhanced *E* region and *D* region ionisation. This may not only be possible with ionospheric scatter but also with ground scatter (H. Yamagishi, private communication, 1999). The length of time during which scatter is lost may also provide information on the time scale of the enhanced ionisation on the propagation paths.

As discussed earlier, ionospheric convection vortices often form near 14–15 MLT during the growth phase. At expansion phase onset the vortex appears to relax as demonstrated in Fig. 5. This relaxation occurred at the same time as an expansion phase onset observed by IMAGE magnetometer stations which were near midnight at this time. Greenwald and co-workers proposed that the relaxation in the convection vortex was more than just coincidence and that it was a manifestation of a global response to the expansion phase onset. This idea would fit with other suggestions that the current systems and convection respond to expansion phase onset on a larger scale than hitherto believed (*e.g.* Opgenoorth and Pellinen, 1998). The exact mechanism for this global response is not yet well understood and the large scale convection observations available with the SuperDARN radars and global auroral imagers from Polar may provide further insight.

Moving now to the response associated with the formation of the substorm current wedge, there are only a few HF coherent scatter radar observations of electric fields at this time. Lewis *et al.* (1998b) reported observations associated with a small substorm, and in particular related the ionospheric current to the plasma flow over the whole substorm interval. At the formation of the substorm current wedge, an increase in the westward electrojet was associated with a slight suppression of the plasma flow. This event occurred in the centre of the current wedge and the suppression of flow may be even higher at the western edge of the current wedge where the auroral luminosity is expected to be higher (Lewis *et al.*, 1998b).

The substorm current wedge forms at expansion phase onset consisting of upward field aligned current in the west and downward field aligned current in the east with a westward electrojet connecting the two (McPherron *et al.*, 1973). Lewis *et al.* (1997) reported the convection response to the formation of the upward field aligned current and this is schematically illustrated in Fig. 7. The panel on the left of Fig. 7 represents the flow in the Halley field of view prior to the expansion phase onset and formation of the substorm current wedge. Here the flow was mainly westward with a small equatorward component at the equatorward portion of the scatter. The panel on the right of Fig. 7 represents the flow around the western upward field aligned current at the time the current wedge forms. The flow was now vortical about the field aligned current. In the
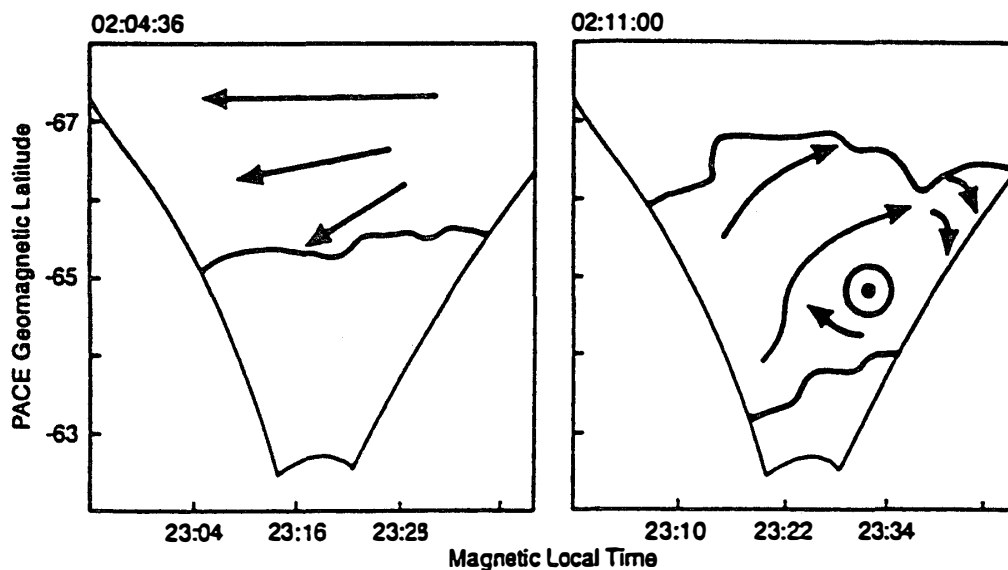
Fig. 7. Sketches of the ionospheric convection just prior to the substorm expansion phase onset (left panel)
and at the time of the formation of the substorm current wedge (right panel) based upon data from
the Halley radar (after Lewis et al., 1997).

poleward part of the field of view the flow direction had changed to eastward while at the
equatorward part the flow was westward. Lewis et al. (1997) emphasise that the actual
flow may have been more complex than the schematic representations in Fig. 7.
Unfortunately the evolution of the flow cannot be followed thereafter as the radar
backscatter disappeared.

5. Expansion phase

The interval following the onset of the expansion phase is very dynamic. The
aurora rapidly moves westward and poleward such that the extent of the substorm
associated aurora can be several hours in MLT and 5–10° in magnetic latitude. There are
also subsequent intensifications of the auroral luminosity which are associated with Pi2
pulsations and enhancements of the westward electrojet. The latter is also often seen to
move poleward and westward in a stepwise fashion.

In the context of the ECPC model, reconnection of open magnetic flux such that the
nightside reconnection rate exceeds the dayside reconnection rate is expected to occur at
or after expansion phase onset. The main consequences of this would be the stimulation
of flows on the nightside and the contraction of the polar cap. If the reconnection takes
place in a bursty fashion then the stimulated flows would most likely appear bursty in the
same way as dayside ionospheric convection responds to flux transfer events (e.g. Elphic
et al., 1990; Neudegg et al., 1999). Returning to Fig. 6 we see that, following the
expansion phase onset at 2024 UT, at the poleward edge of the scatter there were bursts
of enhanced line of sight velocity towards the radar. These pulses of equatorward
velocity occurred after the bite out of radar scatter at the expansion phase onset.
Yeoman and Lühr (1997) demonstrated that these bursts of equatorward velocity were
associated with negative perturbations of the Y component of the magnetic field measured
by the magnetometer at BJO, at a magnetic latitude of ~71°N. Investigation of the full

a Plasma streamlines   b Bx   c By
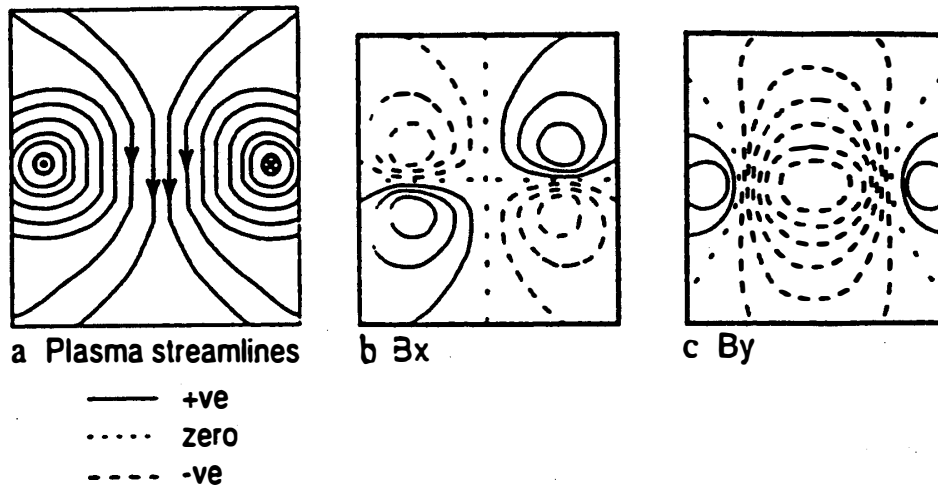
——— +ve
····· zero
- - - -ve

Fig. 8. Plasma streamlines associated with a pair of field aligned currents identified by the up and down arrow symbols, panel a, and the x (north-south) and y (east-west) magnetic field perturbations panels b and c, respectively (after Wei and Lee, 1990).

scan data associated with the pulses indicates that the spatial extent of the pulses was 400–500 km in longitude and 30–400 km in latitude. Careful investigation of the plasma flows and the currents revealed that the features discussed above had similar signatures to the current system associated with a pair of upward and downward field aligned currents as illustrated in Fig. 8 (Wei and Lee, 1990; Yeoman and Lühr, 1997). In this case the upward field aligned current was in the west and the downward field aligned current in the east. The plasma streamlines were equatorward between the two field aligned currents (Fig. 8a). The X and Y magnetic perturbations are then shown in Figs. 8b and 8c, respectively, and the IMAGE magnetometer variations were qualitatively consistent with these perturbations. Having shown that this simple picture can explain the overall nature of the observations, there are then two ways in which the observed temporal variability of the flows may be explained. In one, the pair of currents is essentially stationary and the current density grows and decays with the time. In the second, the temporal variation is a result of the motion of a sequence of current vortices across the radar field of view. If it is the latter then the east-west extent may be larger than suggested above provided the propagation direction is eastward as the radar was scanned from east to west. Taking this into account, the azimuthal extent was ~1000 km and the eastward propagation speed ~5–6 km s^{-1}. In fact the observed signature is probably some combination of both of these possibilities.

The overall characteristics of these impulsive velocity features, such as duration, repetition rate, morphology, are similar to the ionospheric signature of flux transfer events at the dayside magnetopause (*e.g.* Lockwood *et al.*, 1990b). This might imply that they are equivalent signatures of reconnection in the tail. Using the Tsyganenko T89 magnetic field model (Tsyganenko, 1990) these features map to a region 40–-50 R_E downtail and an extent in the Y GSM direction of 10 R_E. If the features do represent the ionospheric signatures of reconnection then they have a voltage of 30 kV and a consequent flux closure rate of ~3 $\times$ 10^4 Wb s^{-1} (Yeoman and Lühr, 1997). This represents a total flux of ~2 $\times$ 10^7 Wb for the complete sequence of events.

Observations of transient flow bursts in the tail, referred to as bursty bulk flows

(BBFs), have been made (*e.g.* Baumjohann *et al.*, 1990; Angelopoulos *et al.*, 1992). Such flow bursts in the tail have similar time scales and intervals and also flux closure rate (Angelopoulos *et al.*, 1992). Coincident measurements by Geotail during the observations of ionospheric flow bursts were reported by Yeoman *et al.* (1998). Geotail, located in the post midnight sector at a radial distance of 10 R_E and ~4 hours to the east of the radar field of view, observed a dawnward perturbation and dipolarisation of the magnetic field and dawnward plasma flow. Yeoman *et al.* (1998) suggested that these tail observations were related to the deceleration of earthward plasma flow and subsequent diversion of the flow during the expansion phase. The exact relationship between the ionospheric and tail signatures remains unclear, however, and needs to be investigated further.

Prior to the enhancements in line-of-sight flow discussed by Yeoman and Lühr (1997) there was a suppression of the flow. Similar reductions in flow were seen with the PACE radar in a separate study (Morelli *et al.*, 1995) and were interpreted as being related to high ionospheric conductivity due to particle precipitation. The flow was suppressed to values between 50 and 100 m s^{-1} but then enhanced rapidly to 0.5–1.0 km s^{-1}. In the case discussed by Morelli and co-workers, the reductions in flow were associated with impulsive, narrow (~300 km) westward electrojets which form poleward of the main substorm westward electrojet. These features then moved equatorward and coalesced with the main electrojet and during this time the flow was enhanced. Estimates of the Hall conductance in the region of suppressed flow ranged from 100 S (Morelli *et al.*, 1995) to 10–40 S (Yeoman and Lühr, 1997), in good agreement with more direct measurements (*e.g.* Lester *et al.*, 1996).

A schematic representation of the flows associated with these electrojets is given in Fig. 9 taken from Morelli *et al.* (1995). The scale sizes of the sketches in Fig. 9 are typically 1000 km in latitude and 1300 km (~2.5 hours of local time) in longitude. In panel a the pre-electrojet onset situation is given with a quasi-steady westward electrojet ~600 km wide and extending many hours in MLT in the lower part. The coincident flows are eastward and equatorward within the electrojet and of order 0.4 km s^{-1} as indicated in Fig. 9a. Figure 9b shows the flows approximately 2 min after the initiation of the electrojet, which was expanding westward at ~1 km s^{-1} and poleward at ~0.5 km s^{-1}. The flow within the new electrojet dropped to ~0.1 km s^{-1} as this region presented an obstacle to the equatorward flow which was diverted around the western edge of the expanding electrojet, producing flows of ~1.0 km s^{-1}. After 4 min (Fig. 9c) the poleward expansion had ceased and there appeared to be a general equatorward motion of the new electrojet into the pre-existing electrojet. The flow, however, was still low within this region but high outside the western edge. The next stage (Fig. 9d) saw the flow within the new electrojet having recovered such that there was a surge of equatorward flow, apart from at the western edge. After 8 min these flows were reduced as the new electrojet had almost completely coalesced with the original electrojet. The processes described above were essentially completed after 9–10 min. This pattern of flow illustrates the complexity of the flow in localised regions during substorms and the need for maps of the flow rather than simple slices through the flow.

The other consequence of the ECPC and reconnection in the tail is the subsequent contraction of the polar cap as the tail reconnection rate exceeds the dayside reconnection
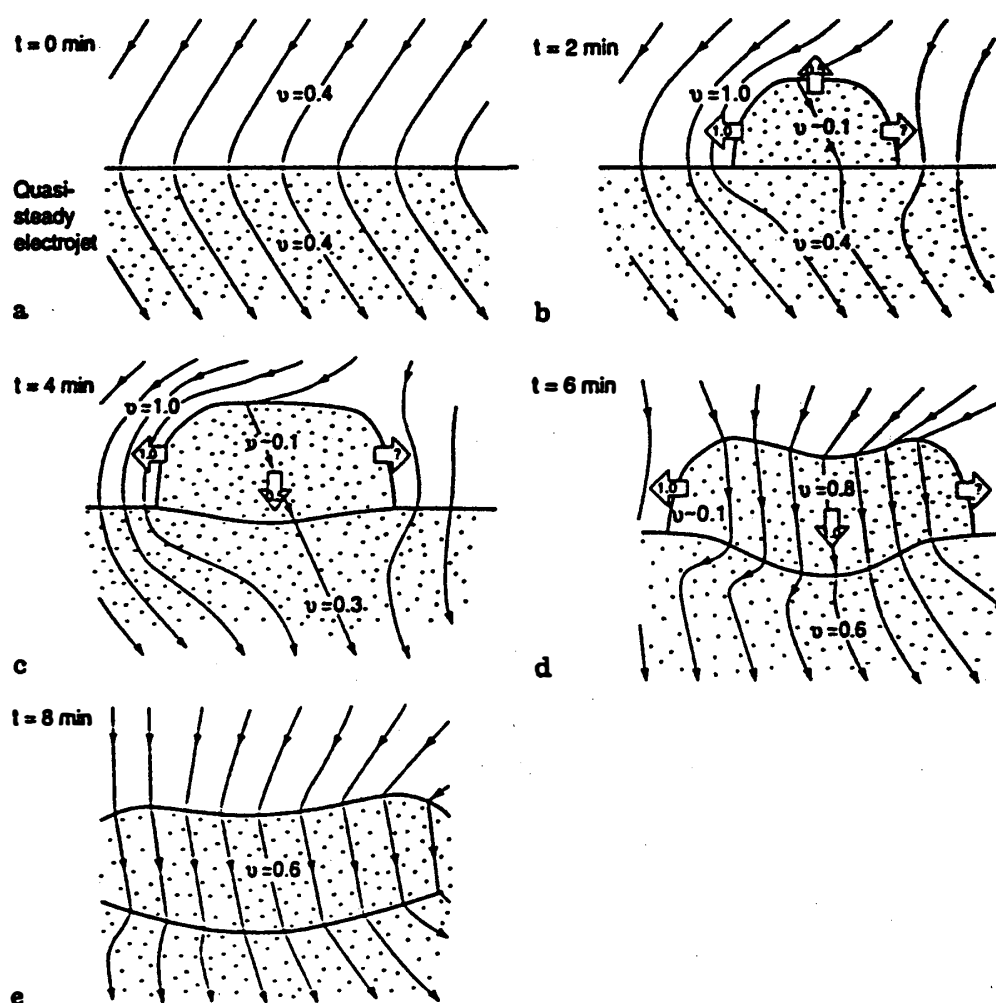
Fig. 9. Sketches of the evolution of impulsive electrojets and the associated plasma flow during late
expansion phase onset (after Morelli et al., 1995).

rate. A number of studies have demonstrated this contraction (*e.g.* Lockwood *et al.*,
1988; Lester *et al.*, 1990; Taylor *et al.*, 1996). Similar observations with HF coherent
scatter radars have been discussed by Yeoman and Pinnock (1996) and in multi-
instrument studies by Fox *et al.* (1994, 1999). Such studies generally use the convection
reversal boundary (CRB) as a proxy for the polar cap boundary. It is normally close to
the PCB, although may generally be slightly displaced to lower latitudes because of the
effect of any viscous driving of convection. Yeoman and Pinnock (1996) demonstrated
the difficulty of this type of study when the IMF B_y component varies. Since the polar
cap boundary is shifted asymmetrically towards dawn or dusk depending upon the sign of
IMF B_y, motion of the polar cap boundary may be caused by changing B_y. Separating
the effects of changing B_y polarity and closure of open magnetic flux in the tail can,
therefore, be difficult during such intervals. Yeoman and Pinnock demonstrated that the
CRB did move poleward, as expected in the ECPC model, but only ~27 min after
expansion phase onset. This delay is in good agreement with other measures of the time
delay between expansion phase onset and the initiation of contraction (*e.g.* Lockwood
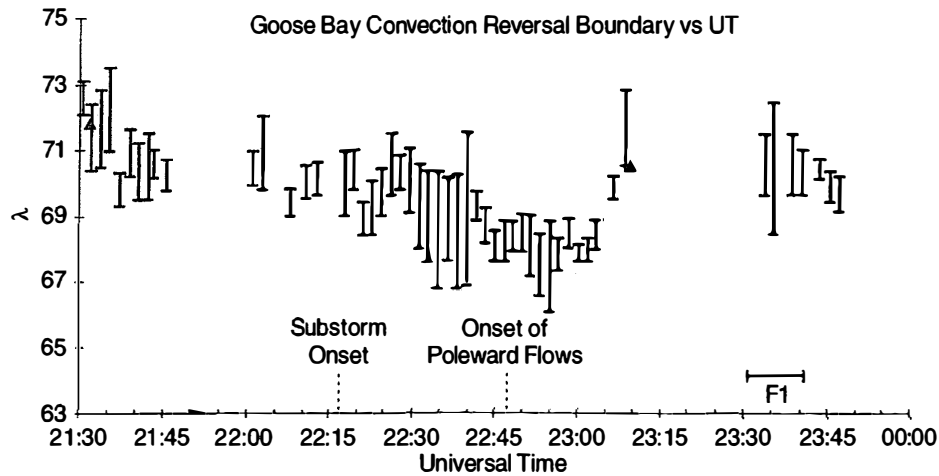and Cowley, 1992; Taylor *et al.*, 1996). The observations were made in the dusk local

Fig. 10. The convection reversal boundary measured by Goose Bay during a period of substorm activity (after Fox et al., 1999).

time sector. The poleward velocity of the CRB was also quite large, 1.7 ± 0.7 km s^{-1} also in good agreement with other observations (e.g. Lester et al., 1990).

Figure 10 (taken from Fox et al., 1999) illustrates the motion of the CRB measured by the Goose Bay radar during a complete substorm interval, including growth, expansion and recovery. Full details of the background to the interval are given in Fox et al. (1999) but the expansion phase onset occurred at 2215 UT. The CRB moved equatorward during the growth phase, as predicted by the ECPC model, and continued to expand following expansion phase onset. There was an intensification of the expansion phase at 2240 UT and following this the CRB remained at an approximately constant magnetic latitude, 68°, until 2305 UT when there was a poleward jump to 72° magnetic latitude. Again it appears that the contraction of the polar cap occurred some time after expansion phase onset. It is important, however, to consider the IMF during the interval as Fox et al. (1999) have done. On this occasion B_z was strongly negative, -20 nT, up to 2235 UT when it turned positive. Fox et al. (1999) suggest the poleward jump of the CRB was a result of the radar moving into a region of flow driven by nightside reconnection whereas prior to this the CRB observed by the radar was located in the viscous cell on closed field lines. After 2305 UT therefore, the observed CRB would have been closer to the open/closed field line boundary.

Importantly both the above studies demonstrate the difficulty of tracking the behaviour of the polar cap boundary, or its proxy the CRB, with one radar alone. It is necessary to have complete information about the whole large scale convection pattern, as well as IMF conditions and substorms indicators, in order to compare observations directly with the predictions made by the ECPC model. Such studies are now starting to appear in the literature (e.g. Pulkkinen et al., 1998) as a consequence of the development of the SuperDARN array.

6. Recovery phase

Discussion of observations by HF radars during the recovery phase is limited. A

number of studies (*e.g.* Yeoman and Lühr, 1997; Fox *et al.*, 1999) present data which occurred during the recovery phase but concentrate on other aspects. One of the problems in discussing the recovery phase is identifying when expansion phase has ended and recovery has begun. The event discussed by Yeoman and Lühr (1997) and which is shown in Fig. 6 is a good example in this respect. The magnetometer data from IMAGE indicate that the magnetic perturbations at SOR and MAS (67.2° and 66.1° magnetic latitude, respectively) caused by the electrojets initiated at expansion phase onset began to decay at 2230 UT. At BJN (71.3° magnetic latitude), however, there was a further intensification of an electrojet, which was further supported by a Pi 2 pulsation observed at mid-latitudes, at 2255 UT. The magnetic perturbation at BJN associated with this electrojet began to decay at ~2315 UT. Returning to Fig. 6, there were a number of features within the data worthy of note after the intensification at 2255 UT. For example, there were 2, possibly 3, further bursts of flow towards the radar, together with some enhancements of flow away from the radar. Also, the flow after 2320 UT was primarily away from the radar, compared with predominantly toward the radar before that. This indicates, as does the flow from the scan data, that the radar observed generally eastward flow, with poleward components. The fact that this occurred at or near the start of the recovery phase is perhaps important and needs further investigation. Another study with EISCAT data in a similar local time sector demonstrated that prior to expansion phase onset the flow was mainly in the dusk cell, while at the start of the recovery phase they were mainly in the dawn cell (Lester *et al.*, 1995). Of course this may simply have been due to the continued rotation of the radar fields of view and it is, therefore, important to establish the overall flow pattern using the SuperDARN radars.

The final comment regarding the recovery phase data in Fig. 6 concerns the location of the radar backscatter. After the final Pi2 pulsations the region of scatter moved rapidly poleward from between 65.5° and 72.5° magnetic latitude to between 71° and 76° magnetic latitude at ~2330 UT, after which the scatter remained at a reasonably constant latitude. Whether this is the recovery phase equivalent to the growth phase signatures discussed earlier is unclear. The average position of the statistical Feldstein auroral oval for $K_p = 1$ (Feldstein and Starkov, 1967), overlaid on Fig. 6, does not predict such a dramatic change during the time scale involved.

Omega bands are a well established optical signature of the recovery phase (Akasofu, 1964). A multi-instrument study, involving data from the CUTLASS Finland radar, has recently been presented by Wild *et al.* (2000). The omega bands discussed in this study occurred during the recovery phase of a substorm which had the expansion phase onset located in the Scandinavian sector. The case study demonstrated that the occurrence of the omega bands in the post midnight local time sector was simultaneous with the onset of a substorm to the west of Scandinavia. Wild *et al.* (2000) suggest that this simultaneous occurrence may have been more than coincidence and that the global response to an expansion phase onset, or intensification, which occurs during the recovery phase of a previous substorm triggers the downward current at the poleward edge of the auroral oval to become unstable. This is perhaps a nightside/recovery phase equivalent signature to the change in the current vortex in the 15 MLT sector discussed earlier (Greenwald *et al.*, 1996). The important point is that the global current circuit may be significantly changed at expansion phase onset and thus leads to the conclusion

that global scale observations are required to investigate this problem further.

7. Summary and conclusions

The above review demonstrates the ability of HF coherent scatter radars to make key observations of ionospheric convection during magnetospheric substorms. Importantly, these systems continue to make observations during all phases of the substorm, and even temporary loss of radar backscatter can be turned to advantage. It is clear from the observations, also, that in contributing to multi-instrument studies of magnetospheric substorms, HF coherent scatter radars play an important role.

The comparison of the observations with predictions made by the ECPC model is in general reasonable. Nevertheless the observations which have been made represent only the start of what can be achieved and there are many important issues which need to be addressed. Some points which need to be considered further have been identified by the observations reported above. Others are more generic, while the continued development of the SuperDARN array will lead to further studies. One example of the former case is the question of whether the equatorward motion of the region of the radar backscatter occurs at times other than following long intervals of northward IMF. If examples can be found, then this could lead to a diagnostic tool whereby the polar cap area and reconnection rate at the dayside magnetopause can be routinely monitored. A second example is the relationship between the flow bursts observed during the late expansion phase, bursty bulk flows in the tail and magnetic reconnection. So far we have tantalising evidence for the relationship but clearly further work needs to be done. Examples of the more generic problems are the differences in flow associated with pseudo break-ups and expansion phase onset, as well as the timing of the polar cap contraction and the excitation of flow due to reconnection of open magnetic flux in the tail. The extension of the SuperDARN array of HF coherent scatter radars lends itself to the study of the global response of the magnetosphere ionosphere system to expansion phase onset. There is evidence from both the post noon sector, where convection vortices change, and the post midnight sector, where omega bands may be initiated, that the system responds in a much more global manner than previously thought. Furthermore, single radar observations of the CRB during substorms can be difficult to interpret correctly and global scale observations will provide far more information than currently discussed.

The next few years offer excellent opportunities to further these studies. The SuperDARN array continues to expand in both hemispheres, the Polar imagers continue to provide high quality global images of the auroral activity during magnetospheric substorms, and new spacecraft will be launched offering multi-point measurements, the Cluster mission, or large scale imaging of the magnetosphere, the IMAGE mission.

thank Prof. N. Sato for his hospitality during a visit to the National Institute of Polar Research (NIPR), Tokyo, which was funded by NIPR. The SuperDARN radars are funded by various research agencies in Australia, Canada, Finland, France, Italy, Japan, Sweden, South Africa, U.K. and U.S.A. The author thanks anonymous referees for their kind comments in reviewing the paper.

The editor thanks Drs. Natsuo Sato and Raymond A. Greenwald for their help in evaluating this paper.

References

Akasofu, S.-I. (1964): The development of the auroral substorm. Planet. Space Sci., **12**, 273–282.

Angelopoulos, V., Baumjohann, W., Kennel, C.F., Coroniti, F.V., Kivelson, M.G., Pellat, R., Walker, R.J., Lühr, H. and Paschmann, G. (1992): Bursty bulk flows in the inner central plasma sheet. J. Geophys. Res., **97**, 4027–4039.

Baker, D.N., Pulkkinen, T.I., Angelopoulos, V., Baumjohann, W. and McPherron, R.L. (1996): Neutral line model of substorms: Past results and present view. J. Geophys. Res., **101**, 12975–13010.

Baumjohann, W., Paschmann, G. and Lühr, H. (1990): Characteristics of high-speed ion flows in the plasma sheet. J. Geophys. Res., **95**, 3801–3809.

Brittnacher, M., Filligam, M., Parks, G., Germany, G. and Spann, J. (1999): Polar cap area and boundary motion during substorms. J. Geophys. Res., **104**, 12251–12262.

Cogger, L.L., Murphree, J.S., Ismail, S. and Anger, C.D. (1977): Characteristics of dayside 5577 Å and 3914 Å aurora. Geophys. Res. Lett., **4**, 413–416.

Cowley, S.W.H. (1984): Solar wind control of magnetospheric convection. Proc. Conf. Achievements of the IMS, **ESA SP-217**, 483–494.

Cowley, S.W.H. (1998): Excitation of flow in the Earth's magnetosphere-ionosphere system: Observations by incoherent scatter radar. Polar Cap Boundary Phenomena, ed. by J. Moen *et al.* Dordrecht, Kluwer Academic Publ., 127–140.

Dungey, J.W. (1961): Interplanetary magnetic field in the auroral zones. Phys. Rev. Lett., **6**, 47–48.

Elphic, R.C., Lockwood, M., Cowley, S.W.H. and Sandholt, P.E. (1990): Flux transfer events at the magnetopause and in the ionosphere. Geophys. Res. Lett., **17**, 2241–2244.

Etemadi, A., Cowley, S.W.H., Lockwood, M., Bromage, B.J.I., Willis, D.M. and Lühr, H. (1988). The dependence of high-latitude dayside ionospheric flows on the north-south component of the IMF: A high time resolution correlation analysis using EISCAT "Polar" and AMPTE UKS and IRM data. Planet. Space Sci., **36**, 471–498.

Evans, D.S. (1985): The characteristics of a persistent auroral arc at high latitudes in the 1400 MLT sector. The Polar Cap, ed. by J. Holtet and A. Egeland. Norwell, D. Reidel, 99–109.

Fejer, B.G. and Kelley, M.C. (1980): Ionospheric irregularities. Rev. Geophys. Space Phys., **18**, 401–443.

Feldstein, Y.I. and Starkov, G.V. (1967): Dynamics of auroral belt and polar geomagnetic disturbances. Planet. Space Sci., **15**, 209–229.

Fox, N.J., Lockwood, M., Cowley, S.W.H., Freeman, M.P., Friis-Christensen, E., Milling, D.K., Pinnock, M. and Reeves, G.D. (1994): EISCAT observations of unusual flows in the morning sector associated with weak substorm activity. Ann. Geophys., **12**, 541–553.

Fox, N.J., Cowley, S.W.H., Davda, V.N., Enno, G., Friis-Christensen, E., Greenwald, R.A., Hairston, M.R., Lester, M., Lockwood, M., Lühr, H., Milling, D.K., Murphree, J.S., Pinnock, M. and Reeves, G.D. (1999): A multipoint study of a substorm occurring on 7 December 1992 and its theoretical implications. Ann. Geophys., **17**, 1369–1384.

Greenwald, R.A., Baker, K.B., Hutchins, R.A. and Hanuise, C. (1985): An HF phased array radar for studying small-scale structure in the high-latitude ionosphere. Radio Sci., **20**, 63–72.

Greenwald, R.A., Baker, K.B., Dudeney, J.R., Pinnock, M., Jones, T.B., Thomas, E.C., Villain, J.-P., Cerisier, J.-C., Senior, C., Hanuise, C., Hunsucker, R.D., Sofko, G., Koehler, J., Nielsen, E.,

Pellinen, R., Walker, A.D.M., Sato, N. and Yamagishi, H. (1995): Darn/SuperDARN; a global view of the dynamics of high-latitude convection. Space Sci. Rev., **71**, 761–796.

Greenwald, R.A., Ruohoniemi, J.M., Bristow, W.A., Sofko, G.J., Villain, J.-P., Huuskonen, A., Kokubun, S. and Frank, L.A. (1996): Mesoscale dayside convection vortices and their relation to substorm phase. J. Geophys. Res., **101**, 21697–21713.

Haldoupis, C. (1989): A review on radio studies of auroral E-region ionospheric irregularities. Ann. Geophys., **7**, 239–254.

Hill, T.W. (1975): Magnetic merging in a collisionless plasma. J. Geophys. Res., **80**, 4689–4692.

Kamide, Y. and Baumjohann, W. (1993): Magnetosphere-Ionosphere Coupling. Berlin, Springer, 178 p.

Kamide, Y. and Kokubun, S. (1996): Two-component auroral electrojet: Importance for substorm studies. J. Geophys. Res., **101**, 13027–14046.

Khan, H. and Cowley, S.W.H. (1999): Observations of the response time of high-latitude ionospheric convection to variations in the interplanetary magnetic field using EISCAT and IMP-8 data. Ann. Geophys., **17**, 1306–1335.

Koskinen, H.E.J., Lopez, R.E., Pellinen, R.J., Pulkkinen, T.I., Baker, D.N. and Bösinger, T. (1993): Pseudo break-up and substorm growth phase in the ionosphere and magnetosphere. J. Geophys. Res., **98**, 5801–5813.

Lester, M., Freeman, M.P., Southwood, D.J., Waldock, J.A. and Singer, H.J. (1990): A study of the relationship between interplanetary parameters and large displacements of the nightside polar cap. J. Geophys. Res., **95**, 21133–21145.

Lester, M., Lockwood, M., Yeoman, T.K., Cowley, S.W.H., Lühr, H., Bunting, R. and Farrugia, C.J. (1995): The response of ionospheric convection in the polar cap to substorm activity. Ann. Geophys., **13**, 147–158.

Lester M., Davies, J.A. and Virdi, T.S. (1996): High latitude Hall and Pedersen conductances during substorm activity in the SUNDIAL-ATLAS campaign. J. Geophys. Res., **101**, 26719–26728.

Lester, M., Milan, S.E., Baker, K., Greenwald, R.A., Brittnacher, M., Lummerzheim, D., Owen, C.J., Pulkkinen, T., Reeves, G.D., Sofko, G. and Villain, J.-P. (1998): Polar, IMP-8 and SuperDARN observations of substorm growth and expansion phase signatures. SUBSTORMS-4, ed. by S. Kokubun and Y. Kamide. Tokyo, Terra Sci. Publ., 175–178.

Lewis, R.V., Freeman, M.P., Rodger, A.S., Reeves, G.D. and Milling, D.K. (1997): The electric field response to the growth phase and expansion phase onset of a small isolated substorm. Ann. Geophys., **15**, 289–299.

Lewis, R.V., Freeman, M.P. and Reeves, G.D. (1998a): The relationship of HF radar backscatter to the accumulation of open magnetic flux prior to substorm onset. J. Geophys. Res., **103**, 26613–26619.

Lewis, R.V., Freeman, M.P., Rodger, A.S., Watanabe, M. and Greenwald, R.A. (1998b): The behaviour of the electric field within the substorm current wedge. J. Geophys. Res., **103**, 179–187.

Lockwood, M. and Cowley, S.W.H. (1992): Ionospheric convection and the substorm cycle. Proc. Int. Conf. On Substorms, ESA SP-335, 99–109.

Lockwood, M., Cowley, S.W.H., Todd, H., Willis, D.M. and Clauer, C.R. (1988): Ion flows and heating at a contracting polar cap boundary. Planet. Space Sci., **36**, 1229–1253.

Lockwood, M., Cowley, S.W.H. and Freeman, M.P. (1990a): The excitation of plasma convection in the high-latitude ionosphere. J. Geophys. Res., **95**, 7961–7971.

Lockwood, M., Cowley, S.W.H., Sandholt, P.E. and Lepping, R.P. (1990b): The ionospheric signatures of flux transfer events and solar wind dynamic pressure changes. J. Geophys. Res., **95**, 17113–17124.

Lockwood, M., Moen, J., Cowley, S.W.H., Farmer, A.D., Løvhaug, U.P., Lühr, H. and Davda, V. (1993): Variability of dayside convection and motions of the cusp/cleft aurora. Geophys. Res. Lett., **20**, 1011–1014.

Lui, A.T.Y. (1996): Current disruption in the Earth's magnetosphere: Observations and models. J. Geophys. Res., **101**, 13067-13088.

McPherron, R.L., Russell, C.T. and Aubry, M.P. (1973): Satellite studies of magnetospheric substorms on August 15 1968. 9. Phenomenological model for substorms. J. Geophys. Res., **78**, 3131–3149.

Milan, S.E., Davies, J.A. and Lester, M. (1999): Coherent HF radar backscatter characteristics associated with auroral forms identified by incoherent radar techniques. J. Geophys. Res., **104**, 22591–22603.

Morelli, J.P., Bunting, R.J., Cowley, S.W.H., Farrugia, C.J., Freeman, M.P., Friis-Christensen, E., Jones, G.O.L., Lester, M., Lewis, R.V., Lühr, H., Orr, D., Pinnock, M., Williams, P.J.S. and Yeoman, T.K. (1995): Radar observations of auroral-zone flows during a multiple-onset substorm. Ann. Geophys., **13**, 1144–1163.

Nagai, T., Fujimoto, M., Saito, Y., Machida, S., Terasawa, T., Nakamura, R., Yamamoto, T., Mukai, T., Nishida, A. and Kokubun, S. (1998): Structure and dynamics of magnetic reconnection for substorm onsets with Geotail observations. J. Geophys. Res., **103**, 4419–4428.

Neudegg, D.A., Yeoman, T.K., Cowley, S.W.H., Provan, G., Haerendel, G., Baumjohann, W., Auster, U., Fornacon, K.-H., Georgescu, E. and Owen, C.J. (1999): A flux transfer event observed at the magnetopause by the Equator-S spacecraft and in the ionosphere by the CUTLASS HF radar. Ann. Geophys., **17**, 707–711.

Opgenoorth, H. and Pellinen, R.J. (1998): The reaction of the global convection electrojets to the onset and expansion of the substorm current wedge. SUBSTORMS-4, ed. by S. Kokubun and Y. Kamide. Dordrecht, Kluwer Academic Publ., 663–672.

Pulkkinen, T.I., Baker, D.N., Frank, L.A., Sigwarth, J.B., Opgenoorth, H.J., Greenwald, R., Friis-Christensen, E., Mukai, T., Nakamura, R., Singer, H., Reeves, G.D. and Lester, M. (1998): Two substorm intensifications compared: Onset, expansion and global consequences. J. Geophys. Res., **103**, 15–29.

Ranta, H. (1978): The onset of an auroral absorption substorm. J. Geophys. Res., **83**, 3893–3901.

Ruohoniemi, J.M. and Baker, K.B. (1998): Large-scale imaging of high-latitude convection with Super Dual Auroral Radar Network HF radar observations. J. Geophys. Res., **103**, 20797–20806.

Siscoe, G.L. and Huang, T.S. (1985): Polar cap inflation and deflation. J. Geophys. Res., **80**, 543–548.

Sofko, G.J., Greenwald, R.A. and Bristow, W.A. (1995): Direct determination of large-scale magnetospheric field-aligned currents with SuperDARN. Geophys. Res. Lett., **22**, 2041–2044.

Sonnerup, B.U.Ö (1974): Magnetopause reconnection rate. J. Geophys. Res., **79**, 1546–1552.

Taylor, J.R., Yeoman, T.K., Lester, M., Emery, B.A. and Knipp, D.J. (1996): Variations in the polar cap area during intervals of substorm activity on March 20–21, 1990 deduced from AMIE convection patterns. Ann. Geophys., **14**, 879–887.

Tsyganenko, N.A. (1990): Quantitative models of the magnetospheric magnetic field: methods and results. Space Sci. Rev., **54**, 75–104.

Wei, C.Q. and Lee, L.C. (1990): Ground magnetic signatures of moving elongated plasma clouds. J. Geophys. Res., **95**, 2405–2418.

Wild, J.A., Yeoman, T.K., Eglitis, P. and Opgenoorth, H. (2000): Multi-instrument observations of the electric and magnetic field structure of omega bands. Ann. Geophys., **18**, 99–110.

Yeoman, T.K. and Pinnock, M. (1996):The high latitude convection response to an interval of substorm activity. Ann. Geophys., **14**, 518–530.

Yeoman, T.K. and Lühr, H. (1997): CUTLASS/IMAGE observations of high-latitude convection features during substorms. Ann. Geophys., **15**, 692–702.

Yeoman, T.K., Mukai, T. and Yamamoto, T. (1998): Simultaneous ionospheric and magnetospheric observations of azimuthally propagating transient features during substorms. Ann. Geophys., **16**, 754–763.

Yeoman, T.K., Lewis, R.V., Milan, S.E. and Watanabe, M. (1999): An interhemispheric study of the ground magnetic and ionospheric electric fields during the substorm growth phase and expansion phase onset. J. Geophys. Res., **104**, 14867–14876.